Relaxation Times and Basic Pulse Sequences

An Offprint from

Peter A. Rinck

Magnetic Resonance in Medicine

A Critical Introduction

The Basic Textbook
of the European Magnetic Resonance Forum

13th edition • 2021
335 figures, 36 tables

Peter A. Rinck
Magnetic Resonance in Medicine • A Critical Introduction
The Basic Textbook of the European Magnetic Resonance Forum
13th edition 2021 – www.magnetic-resonance.org • www.trtf.eu • centralmaildesk@trtf.eu

European Magnetic Resonance Forum is an imprint of
THE ROUND TABLE
FOUNDATION

First English edition 1985
Eleventh English edition (e-book) 2017
Twelfth English edition (print) 2018
Thirteenth English edition (print) 2021

A bibliographic entry has been prepared for the Deutsche Nationalbibliographie. The German National Library (Deutsche Bibliothek) lists this publication in the German National Bibliography; detailed bibliographic data are available in the internet.

The interludes between the chapters were taken from Rinckside (ISSN 2364-3889). Rinckside is published at least six times per year both in an electronic (www.rinckside.org) and a printed version. Rinckside is listed by the German National Library.

Medicine and the sciences are ever-changing disciplines. Research and clinical experience are continually broadening our knowledge, in particular the knowledge of proper treatment and use of pharmaceuticals. Insofar as this book mentions any dosage or application, or proposes certain imaging, pharmaceutical applications, spectroscopy or other procedures, readers may rest assured that the author and Foundation have made every effort to ensure that such references are strictly in accordance with the state of knowledge at the time of production.

Some of the product names, patents, and registered designs referred to in this book are in fact registered trademarks or proprietary names even though specific reference to this fact is not always made in the text. Therefore, the appearance of a name without designation as proprietary is not to be construed as a representation that it is in the public domain.

Printing, binding and distribution in the DACH countries:
BoD Book on Demand, Norderstedt, Germany. Printed in Germany.
ISBN: to be announced – preprint – VII3

Foreword

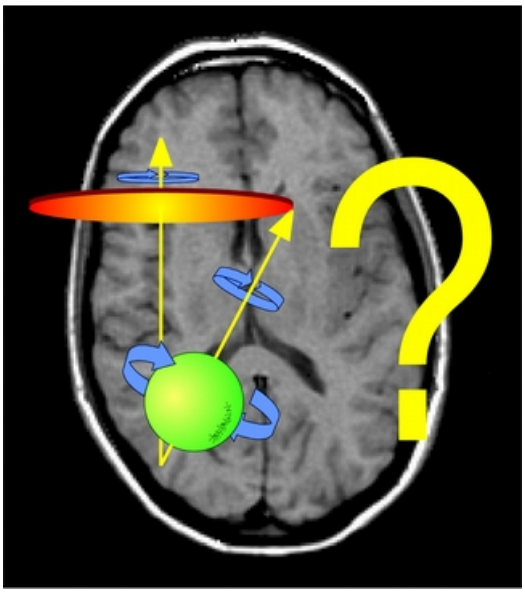

"Why, sometimes I've believed as many as six impossible things before breakfast."
The White Queen in Lewis Caroll's
'Alice Through the Looking Glass'.

We like books – printed on paper, if possible with a beautiful hard-cover binding. Thus, putting this standard textbook on the internet some years ago was a challenge. Now we return with a printed version of the magnetic resonance textbook. The reasons I have described elsewhere.[1]

Celebrating the 50th anniversary of MR imaging in 2021 was a good occasion to publish a new edition. The textbook-child has grown up, become an adult or, in our case – a rather successful standard textbook. The reviews and public reaction to the book were extremely positive.

The first version of this primer – a little booklet – was written at Paul C. Lauterbur's laboratories in the early 1980s. Lauterbur was the father of MR imaging and received the Nobel Prize twenty years later. The text was intended to be used as the Basic Textbook for EMRF, the European Magnetic Resonance Forum. After Lauterbur saw the first edition, he commented: "It looks like a fine book, especially for residents, nurses, and technicians."

Initially we thought this statement was not very encouraging, but in hindsight this was exactly what we had intended to write. We worked on it for another twenty years – and finally Lauterbur found the last edition he read before his death "gratifying". How-

1 Rinck PA. An expensive dilemma: Tablets versus textbooks. Rinckside 2015; 26,7: 17-19.

ever, the target audience today includes scientists and university professors. They should be able to acquire a basic knowledge which enables them to pursue studies of their own and to cope with some of the most common problems, among them tissue relaxation, image contrast and artifacts or questions concerning possible hazards to patients – and to become aware of how to perform reliable research, and to ask and be critical.

The main author and the contributors have not attempted to cover the field completely nor to be exhaustive in the topics discussed, as the field of magnetic resonance still is in a permanent stage of development and therefore changing year by year. Clinical MR machines and even equipment sold for scientific purposes have been increasingly altered into push-button black boxes with pre-fab, given and unchangeable protocols. We are not interested in certain gadgets or "apps" of commercial machines, and won't mention or describe them. We try to explain the fundamentals any user should know and understand.

As with everything in life, MR imaging does not only require knowledge of facts but also of background information and of the historical development of the field for critical decision making. Therefore we have interspersed some subjective, critical, and opinion-oriented sections – interludes – intended to offset the technical nature of the teaching sections and provide some insights into more practical questions faced by MR users.

Most of them were taken from *Rinckside* (www.rinckside.org), a collection of columns published since 1990.

Many of the recent developments concerning MR equipment and its medical and biological applications have turned away from magnetic resonance itself to novel engineering and software approaches in image processing including artificial intelligence. Techniques, ideas and algorithms were imported from fields outside medicine and adopted by software engineers with little or no background in MR and medicine nor insight into medical needs. We mention some of the prime approaches without going into details of signal or image processing – they are of no importance for the understanding of fundamental facts of magnetic resonance imaging.

There has been a long list of contributors to this and earlier versions (see page 418). Their support, ideas, dedication, and feedback have added much to the quality of this work. This book was peer-reviewed by a number of competent reviewers in different fields whom I thank for their efforts.

If you want to learn something about magnetic resonance imaging or its applications choose your topic of interest. If you want to learn it from scratch start with Chapter 1; and if you want to air your brain, read the interludes that are scattered in between.

If you find any mistakes in this book, rest assured that they were left intentionally so as not to provoke the gods with something which is perfect. Still, we would be happy about your feedback. We hope that this textbook will be useful for you and that you will enjoy it. If you have comments or suggestions, please write to us.

Peter A. Rinck, June 2021

Contents

Chapter Four

Relaxation Times and Basic Pulse Sequences

Figure 04-01:
Spinning away into dreams: you may need relaxing times to understand relaxation times. But how long will you stay in this position of low energy when the waves start hitting you?

T1: The Spin-Lattice Relaxation Time

Excitation of an equilibrium system always transfers the system to an unstable state of high energy. The length of time the system will remain there depends on the local conditions (Figure 04-01).

For a system of spin nuclei in a magnetic field, an unstable situation is created by a *wave*: the excitation pulse — the system is 'pumped up' with energy supplied by the RF pulse. At the molecular level, the return to equilibrium depends on the local magnetic and electric conditions at the excited nuclei.

If an isolated proton is left excited in absolute vacuum in the absence of any sort of electromagnetic fields, several years might be needed before the nucleus could, by itself, spontaneously return to the equilibrium state of low energy. However, if the proton is surrounded by water, this process can be 'stimulated' by the surrounding nuclei and will then require only a few seconds.

We need a *resonance* to exchange energy from the external world to the spin system. The excited spin system needs to be exposed to electromagnetic fields oscillating with a frequency at or close to the Larmor frequency of the nuclei before it can relax. The relaxation corresponds to the excess nuclei, which were transferred to the

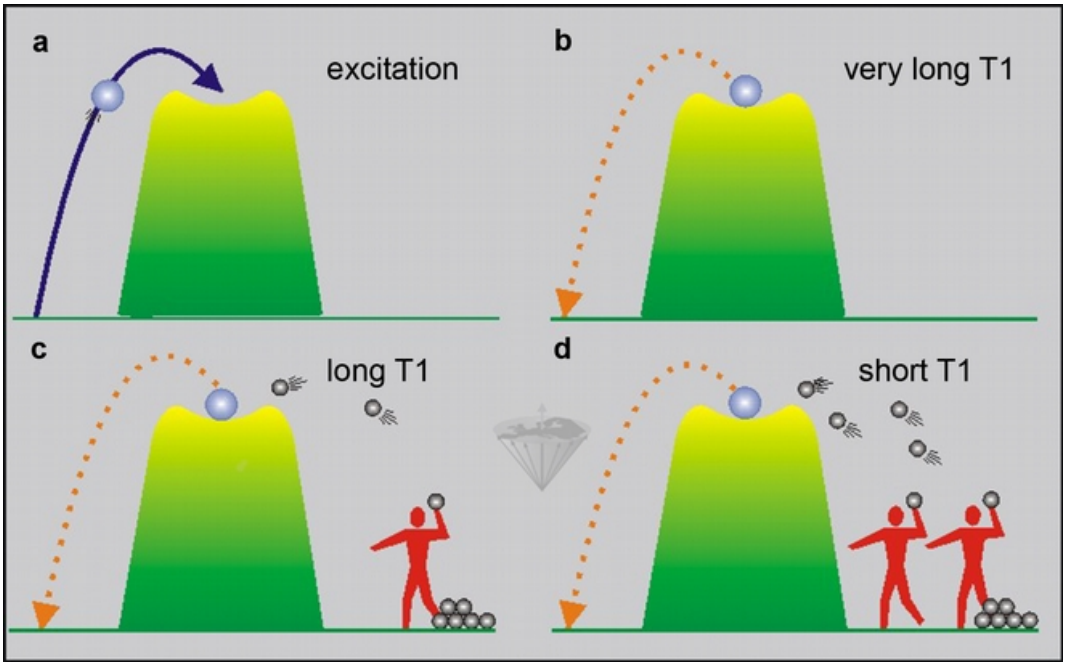

Figure 04-02:
(a) and **(b):** A ball is stuck on top of a small hill (unstable high state of energy).
(c) and **(d):** If two boys try to get it down by throwing rocks at it, on statistical grounds, it will take less time for two boys to achieve their goal compared with one boy.

upper energy level returning to the lower energy level (Figure 02-06 and Figure 04-02). Table 04-01 gives an overview of the different phenomena the system is or can be exposed to while returning to its equilibrium.

The first process of returning to the equilibrium from an excited state is called the *spin-lattice relaxation process* or *longitudinal relaxation process*. It is characterized by the T1 relaxation time. The T1 relaxation time is the time required for the system to recover to 63% of its equilibrium value after it has been exposed to a 90° pulse.

For a given kind of nucleus, T1 depends on several parameters:

- type of nucleus;
- resonance frequency (field strength);
- temperature;
- mobility of observed spins (microviscosity);
- presence of large molecules;
- presence of paramagnetic ions or molecules.

Relaxation Processes	
T1 **('T-one')**	... is the **spin-lattice or longitudinal relaxation time**; the characteristic time constant for spins to tend to align themselves with the **external magnetic field**. Starting from zero magnetization in the z direction, the z magnetization will grow to 63% of its final maximum value in a time T1.
T2 **('T-two')**	... is the **spin-spin** or **transverse relaxation time**; the characteristic time constant for loss of phase coherence among spins oriented at an angle to the **static magnetic field**. It arises from interactions between the spins, with a resulting loss of transverse magnetization. The *x-y* magnetization will decay so that it loses 69% of its initial value in a time T2.
T1-ρ **('T-one-rho')**	... is the **spin-lattice relaxation time in the rotating frame**; the characteristic time constant for loss of magnetization of spins under the influence of a spin-locking B_1 field. Despite its name, T1-ρ relaxation is more closely related to T2 relaxation than T1. If one applies a long lasting B_1 magnetic field immediately after a 90° pulse, the dephasing of the spins in the *x-y* plane is stopped while the B_1 field is on. This is called *spin-locking* and the B_1 field is called a *spin-locking pulse,* even though it may last hundreds of milliseconds. T1-ρ will not be discussed in detail in this introduction to magnetic resonance imaging.

Table 04-01:
The different relaxation processes. T1 and T2 are the important relaxation times for MR imaging.

The presence of large molecules or of paramagnetic ions or molecules is of special interest. In pure water, the process of reorientation (translational movement, rotation, etc.) of a single water molecule occurs very rapidly. Since each molecule has its own magnetic field, this rapid reorientation results in a fluctuating magnetic field at neighboring nuclei.

To promote relaxation, the frequency of the reorientation must be at, or close to, the resonance frequency in pure water. If the frequency of this reorientation is much higher than the Larmor frequency of the protons the relaxation is inefficient.

However, if we add more slowly moving large molecules such as proteins to the water, the water molecules will interact with them. The interaction involves temporary attachment of the water to the proteins and subsequent release. This temporary bonding radically reduces the frequency with which the water molecules reorientate themselves. Pure water, i.e., water in the bulk phase, moves much faster than water close to macromolecules or membranes.

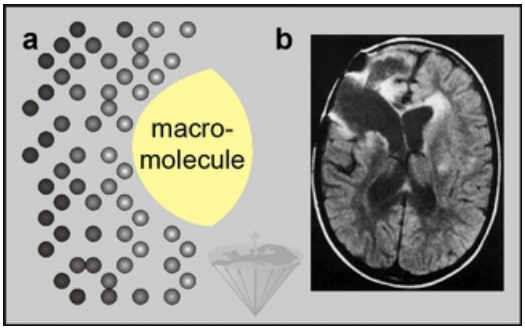

Figure 04-03:
(a) The lower the molecular motion, the shorter the relaxation time T1 (increase in brightness). **(b)** T1-influenced image after a brain tumor operation. Fluid-filled areas are dark, edematous areas are bright: bulk water moves faster, protein-bound water in brain edema slower (shorter T1).

The slower the molecular motion, the shorter the relaxation times T1 (and T2), shown in Figure 04-03 as an increase in brightness.

To characterize the motion of a molecule, the *correlation time* (t*c*) is used. It measures the minimum time required for a molecule to re-orientate itself.

Because of the presence of protein surfaces, the T1 relaxation times of water in living tissue are always shorter than those obtained for pure water. Table 04-02 lists some representative T1 values of normal tissues.

T1 values vary with magnetic field strength. This influences image contrast in MR imaging so that it is not possible to make direct quantitative comparisons between T1 values at different fields. Thus, it is necessary to always mention the field strength when quoting T1 values.

T1 data of brain tissues at different fields are shown in Figure 04-04 (more details can be found in Chapter 10).

Tissue | Organ: T1 Relaxation Times	
Brain	
Gray matter	450 ms
White matter	350 ms
CSF	1500 ms
Heart	
Myocardium	380 ms
Abdomen	
Liver	380 ms
Pancreas	460 ms
Spleen	650 ms
Kidney	
Renal medulla	680 ms
Renal cortex	570 ms
Bowel (wall)	300 ms
Testes	880 ms
Muscle	500 ms
Fatty tissue	230 ms
Bone marrow	490 ms
Skin	320 ms

Table 04-02:
T1 values of some human tissues measured on an MR imaging system at 0.15 Tesla. The standard deviation of these values can be between 10 and 30%; in general, relaxation time values measured *in vivo* are not very reliable.

The data for this figure was acquired with a special NMR equipment dedicated to *relaxometry*. This subdiscipline of NMR deals with the relaxation behavior of different substances. With a *field-cycling relaxometer*, *ex vivo* or *in vitro* measurements of the relaxation behavior of tissue samples or contrast-enhancing compounds can be performed at high accuracy at any field strength; thus identical samples can be examined under identical conditions.

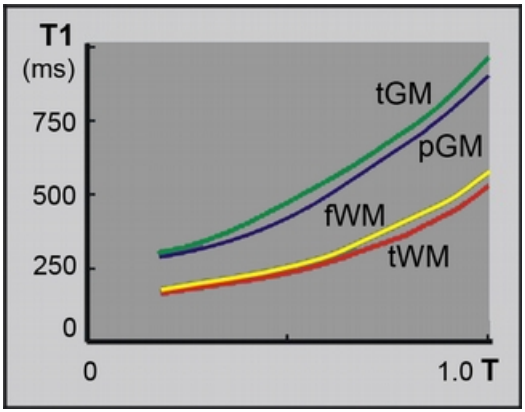

Figure 04-04:
Change of T1 relaxation times of gray and white matter versus field strength. Temporal gray matter (tGM) is depicted green and parietal GM (pGM) is blue; frontal white matter (fWM) is depicted yellow, temporal WM (tWM) is red. T = field in log Tesla.

Field-cycling relaxometry showed that T1 increases nonuniformly with field, leading to specific 'fingerprints' of T1 increase for different tissues.[26] However, due to the complexity of the method, such fingerprints or biological markers have only limited scientific and no clinical diagnostic relevance

Fast Field-Cycling (FFC) can also be used as an imaging technique that exploits varying magnetic fields to quantify molecular motion, providing non-invasively structural information. It might have a certain potential for FFC-NMR biomarkers in medical applications.[27]

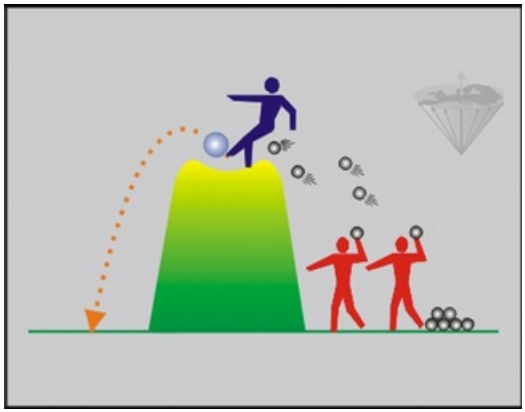

Figure 04-05:
The boys of Figure 04-02 have invited another boy (called "Gadolinium'). His presence on top of the hill kicking the ball down significantly shortens the time the ball would stay in the unstable state.

The explanation as to how the *presence of paramagnetic ions or molecules* can enhance the relaxation rate of water is highly complex. Electrons produce a much stronger magnetic field than nuclei, but when pairing of electrons occurs, there is only a weak net field.

Paramagnetic compounds influence excited spins in a similar way and shorten T1. They have unpaired electrons; their reorientation produces a very strong fluctuating magnetic field, resulting in a significant reduction in the relaxation time (Figure 04-05).

Typical paramagnetic substances include Mn^{2+}, Cu^{2+}, Fe^{2+}, Fe^{3+}, Gd^{3+}, as well as molecular oxygen and free radicals. In certain circumstances, the ability of paramagnetic compounds to alter relaxation rates can be utilized to change the contrast in magnetic resonance images; for this purpose, for instance gadolinium and manganese complexes are used as magnetic resonance contrast agents (see Chapter 13).

26 Rinck PA, Fischer HW, Vander Elst L, Van Haverbeke Y, Muller RN. Field-cycling relaxometry: medical applications. Radiology 1988; 168: 843-849.

27 Broche LM, Ross PJ, Davies GR, MacLeod M-J, Lurie DJ. A whole-body Fast Field-Cycling scanner for clinical molecular imaging studies. Sci Rep. 2019 Jul 18; 9(1): 10402. doi: 10.1038/s41598-019-46648-0.

T1 on the Microscopic Scale

The relaxation times of pure substances, for instance water, can be easily explained.

A living system, however, contains a large number of chemical components, all of which contribute to the observed proton magnetic resonance signal. These components possess different relaxation times. Thus, the analysis of the observed NMR signal in terms of the different subsystem parameters (concentration and relaxation times) is complex but very important.

For the sake of simplicity, we will deal with T1 only in two-component systems. A similar discussion is possible for T2. For example, T1 of muscle tissue protons obtained at 0.1 Tesla is about 300-400 ms, but more than three quarters of the received proton signal stems from water protons, which in the pure liquid show a T1 of several seconds.

Using an example from clinical routine, cerebrospinal fluid (CSF) has similar relaxation times as water. Brain edema, which reflects pathologically high water content in brain tissue, possesses relaxation times that are closer to brain tumors than to CSF (Figure 04-03).

What is the reason for this discrepancy?

This is best explained using the relaxation rate R1. R1 equals 1/T1. Different R1 components can be added to each other to create a new R1 (cf. Chapter 12, page 231).

The T1 of a biological sample is a parameter reflecting the physical and chemical properties in the environment of the observed nuclei. If the environment is not the same throughout the sample, then the obtained T1 will only reflect the mean properties of the sample. In most tissues, one component, usually water, dominates the relaxation behavior. In special cases, where two components with significantly different T1 values are present in comparable amounts, a complex situation arises, which makes a quantitative interpretation difficult.

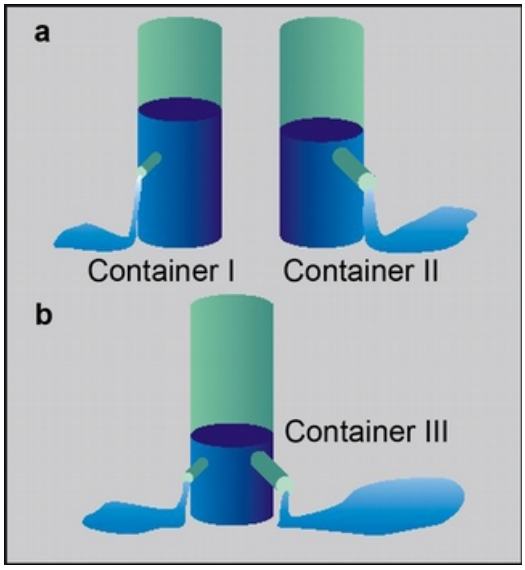

Figure 04-06:
The container example explains the use of relaxation rates instead of relaxation times in a complex system.
(a) Two containers I and II with differently sized outlets;
(b) one container with two differently sized outlets.

Let us consider two systems containing two different groups of protons, one moving fast, one moving slower. Both possess different T1 relaxation times and thus different R1 relaxation rates. We can compare them with the example in Figure 04-06. Here we have two containers, I and II, filled with water. Both of them have an outlet, but the

outlet of Container II is larger than that of Container I (Figure 04-06a). The rate, R, at which water is leaving I and II can be expressed in milliliters per second, and the time needed to empty the containers is given by V/R, where V is the volume of the water (assuming that the water pressure is constant).

If we construct another container (Container III) with volume V and equip it with two outlets (Figure 04-06b), one similar to the outlet of Container I and one similar to the outlet of Container II, then the water in this container will leave at a rate which is the sum of the two outlet rates.

This reflects the relaxation time of a tissue composed like our example in Figure 04-03. Although we have two different components, we only measure one common relaxation time for this tissue.

If the exchange rate between the two groups of protons is very slow or absent, we can identify two different contributions to the relaxation behavior. A physical reason for such a behavior can be found, for example, in samples containing both fat and muscle tissues. The fat cannot exchange protons with the water in the muscle tissue. In the case of slow proton exchange, the system will show *double exponential relaxation*. Other biological systems can show a *single exponential relaxation* behavior, as if they were relaxing governed by a single relaxation time.

It is possible to distinguish the data, provided that enough data points are available. However, the accuracy actually needed for such measurements is often underestimated, in particular in whole-body imaging machines.

Cross Relaxation

Solids, such as proteins and membranes, have a wide range of resonance frequencies, which allows for energy exchange between different parts of the solid. The process of energy exchange in a solid is referred to as *spin diffusion*. Thus, if part of the solid relaxes more rapidly than the rest, it can enhance the relaxation of the whole solid.

A similar process can occur between solids and bound water molecules, with the presence of solids (such as proteins and membranes) in tissue acting to reduce the observed relaxation time for water. This process is described as *off-resonance irradiation* and can be exploited to enhance contrast (*magnetization transfer contrast;* cf. page 205).

T1 on the Macroscopic Scale: Pulse Sequences

To recapitulate: the T1 relaxation time is the time required for the system to recover to 63% of its equilibrium value after it has been exposed to a 90° pulse. To measure this time, several different radio frequency pulse sequences can be employed.

The Partial Saturation Pulse Sequence

This pulse sequence is the most simple sequence in magnetic resonance. It is also called *saturation recovery pulse sequence*, although the latter sequence differs from partial saturation by longer repetition times.

If at time zero, the equilibrium magnetization M_0 is exposed to a 90° pulse, it will be tipped down into the *x'-y'* plane. After a delay time, called *repetition time (TR)*, the spin system is exposed to a second 90° pulse (Figure 04-07), which brings the magnetization down in the *x'-y'* plane where the FID can be monitored.

If TR is equal to or greater than 5×T1, the magnetization in the x'-y' plane is equal to M_0. However, if TR is comparable to T1, relaxation will be incomplete, leading to an observable magnetization smaller than M_0 (Figure 04-08).

The time dependence of Mz (the z-magnetization which equals the signal intensity) on TR, Mz(TR), can be studied by introducing a range of fitting repetition times TR. In the simplest case, the return to equilibrium is a mono-exponential function:

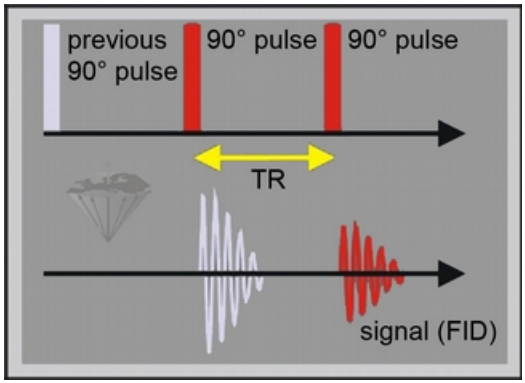

Figure 04-07:
Pulse sequence diagram of a partial saturation sequence, consisting of 90° pulses.
The time between the pulses is called *repetition time*, *TR*. When TR is not long enough for the spins to return completely to the equilibrium (i.e., TR < 5×T1), the signal intensity of the FID is lower than the maximal signal intensity possible.

$$Mz(TR) = Mz(0)\ (1 - \exp[-TR / T1])$$

Thus, it is understandable that if the system is being re-excited at a repetition time TR smaller than 5×T1, the recorded magnetization is less than the maximum value M_0. How much less depends on the ratio of TR over T1.

This effect can be utilized to great advantage if different substances in a given sample have different T1 values. It is possible to reduce part of the signal emerging from the sample, for instance to suppress the signal emerging from fatty tissue.

Also, different samples respond very differently to a train of equidistant 90° pulses (Figures 04-09 and 04-10). This is the basis for TR-influenced contrast behavior in MR imaging.

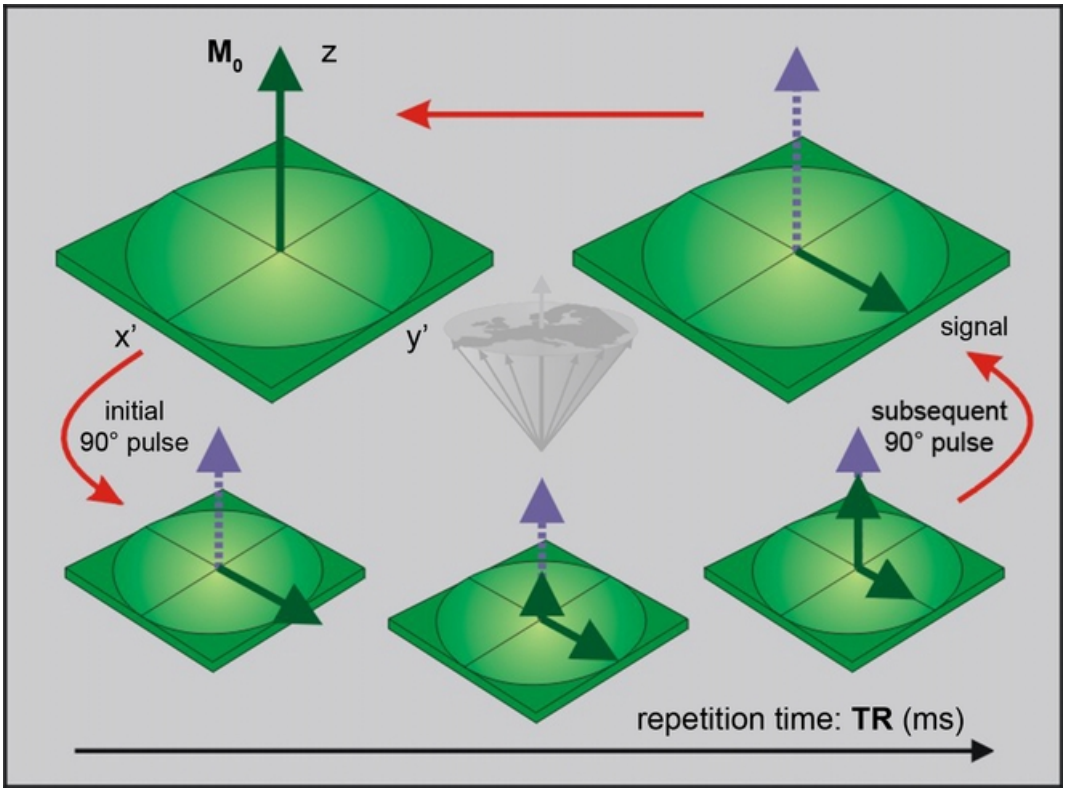

Figure 04-08 (top):
Partial saturation sequence: The magnetization M_0 is tipped by a 90° pulse.
During the repetition time, TR, the system will relax and magnetization will start its return to the equilibrium state. To monitor the size of the magnetization, the system is exposed to a second 90° pulse.

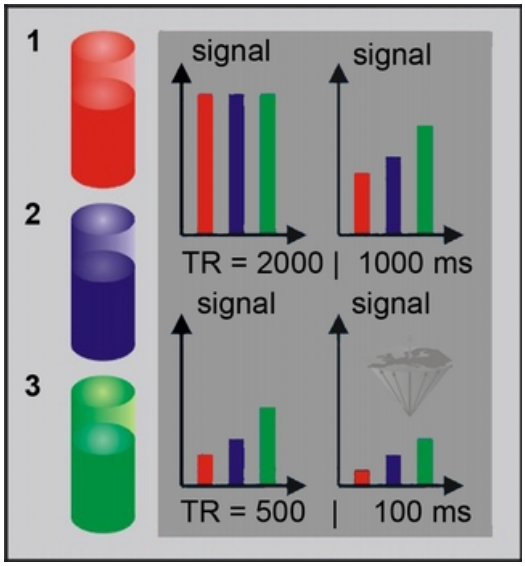

Figure 04-09 (right):
Three different samples, **(1)** blood, **(2)** muscle, and **(3)** fat, assumed to have identical amounts of hydrogen but decreasing relaxation times, are exposed to a train of pulses with different repetition times TR. Note that the blood sample shows the most pronounced saturation behavior, since it has the longest T1.

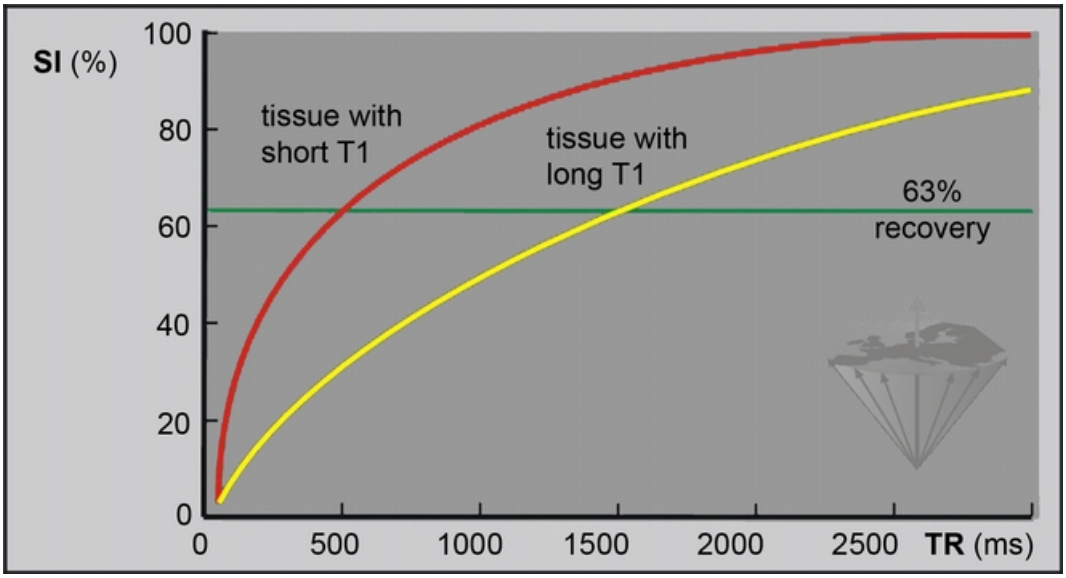

Figure 04-10:
The relative signal intensity (SI) in a partial saturation experiment. TR is the repetition time between two 90° pulses. Two different tissues with T1 relaxation times of 500 and 1,500 ms, respectively, are shown. The signal recovery is 63% after a period of T1.

Partial saturation as described here is only used in a modified form in clinical imaging, namely with the incorporation of a gradient echo. This corresponds to a FLASH imaging sequence which will be discussed at a later stage.

The Inversion Recovery Pulse Sequence

If a spin at equilibrium is subjected to a 180° pulse, the sum magnetization M_0 is inverted with respect to the direction of the external field and becomes antiparallel to the main magnetic field.

Following the inversion, the magnetization starts to recover towards its equilibrium state. The recovery rate is determined by T1.

If we expose the system to a 90° pulse after a certain delay time, the *inversion time TI*, the actual magnetization Mz(TI) will become observable in the *x′-y′* plane as an FID.

By applying a range of different delay times, the time dependence of magnetization, and thus the signal of the inversion time, can be studied in detail. Once again, after a delay time of approximately 5×T1, the magnetization is back to equilibrium.

This 180°-90° pulse sequence is called an *inversion recovery sequence* (Figures 04-11 and 04-12).

In the simplest case, the return to equilibrium is a mono-exponential function:

$$Mz(TI) = Mz(0)\ (1 - 2 \times \exp(-TI / T1))$$

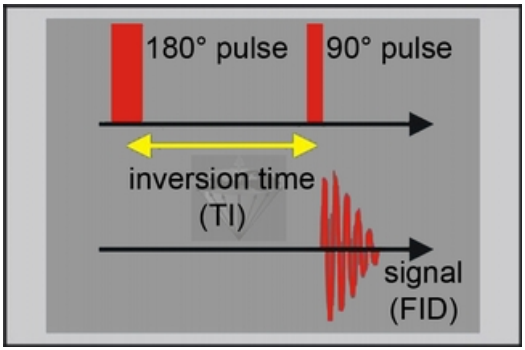

Figure 04-11:
Pulse sequence diagram of an inversion-recovery sequence.
The 180° inversion pulse inverts the magnetization. During the inversion delay (TI), the magnetization recovers at a rate determined by the T1 of the sample. At a certain point during recovery, a 90° pulse is applied and the resulting signal is measured.
The time between the 180° pulse and the following 180° pulse is called *repetition time, TR* (not shown on this graph).

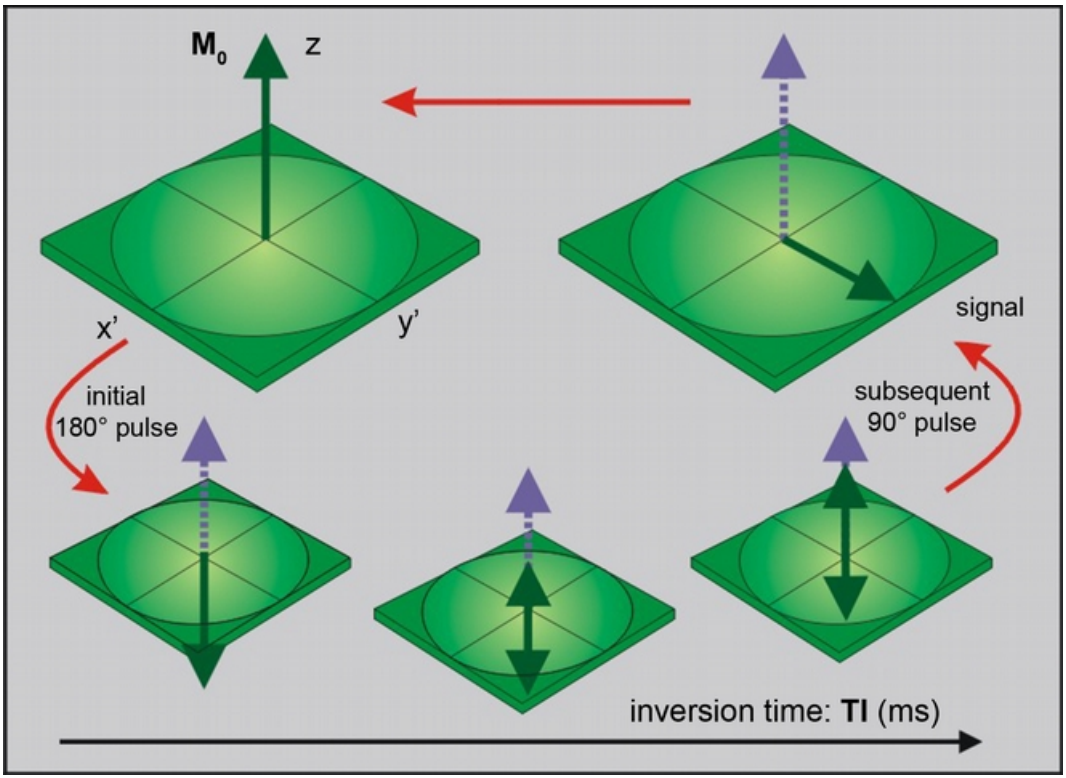

Figure 04-12:
Inversion-recovery sequence: The magnetization is inverted by a 180° pulse.
During the delay time TI, the system will relax and magnetization will start its return to the equilibrium state. To monitor the size of the magnetization, the system is exposed to a 90° pulse, which tips the magnetization into the x'-y' plane and converts the magnetization into signal.

The development of the signal intensity is depicted in Figure 04-13. When TR is not long enough for the spins to return completely to the equilibrium (i.e. TR < 5×T1), the signal intensity (SI) is lower than the maximal intensity possible.

The relative SI measured in an IR experiment is a function of TI, the time between the 180° pulse and the 90° pulse. As with the partial saturation pulse sequence, signal intensity also depends on the repetition time TR. In the case of the IR sequence, the repetition time is the time between the 180° pulses.

It is advisable to choose a TR at least 3×T1 of the tissue of interest to allow for recovery of the longitudinal relaxation of that tissue, thereby avoiding a reduction in signal intensity.

In analytical chemistry, inversion-recovery is applied as a 180°-90° pulse sequence; the initial amplitude of the FID is proportional to the value of the net magnetization at the time of the measurement.

In MR imaging, the sequence is commonly adjusted to the needs of creating an image and, for instance, combined with a spin-echo pulse sequence (cf. page 80).

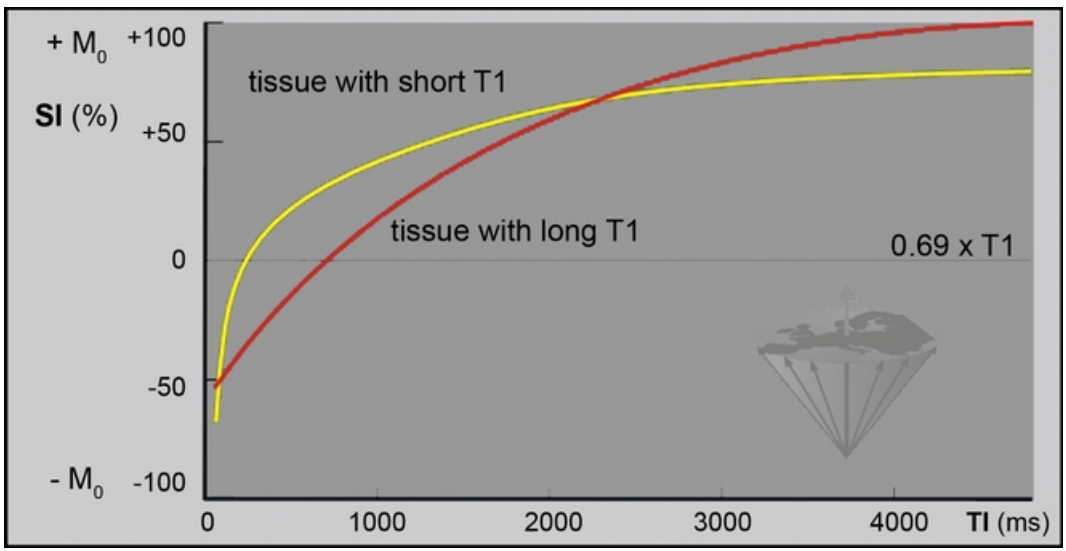

Figure 04-13:
The relative SI measured in an IR experiment as a function of TI, the time between the 180° pulse and the 90° pulse. Note that Mz = 0 for TI = 0.69×T1 (in this example two tissues with T1 = 500, ρ = 72% and 1500 ms, ρ = 100%; TR = 2000 ms).

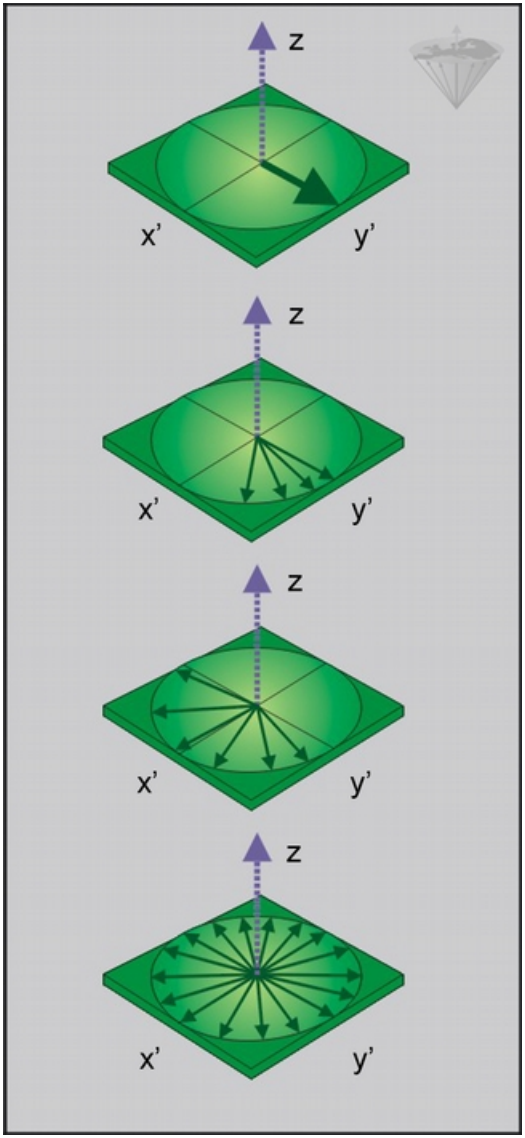

Figure 04-14:
Transverse relaxation phenomena induce an increase in dephasing of individual spins, so a progressive decrease of the macroscopic magnetization is observed.

T2: The Spin-Spin Relaxation Time

After a spin system has been excited by an RF pulse, it initially behaves like a coherent system; i.e., all microscopic components of the macroscopic magnetization precess in phase (all together) around the direction of the external field. However, as time passes, the observed signal starts to decrease as the spins begin to dephase (Figure 04-14).

The decay of the signal in the x'-y' plane is faster than the decay of the magnetization along the z-axis. This additional decay of the net magnetization in the x'-y' plane is due to a loss of phase coherence of the microscopic components, which partly results from the slightly different Larmor frequencies induced by small differences in the static magnetic fields at different locations of the samples.

This process is characterized by T2, the *spin-spin* or *transverse relaxation.*

T2 is dependent on a number of parameters:

- resonance frequency (field strength), although for T2 this is less crucial than for T1 at low, medium, and high (but seemingly not ultrahigh) fields;
- temperature;
- mobility of the observed spin (microviscosity);
- presence of large molecules, paramagnetic ions and molecules, or other outside interference.

In *mobile fluids*, T2 is nearly equal to T1, whereas in solids or in slowly tumbling systems (i.e., high-viscocity systems), static-

field components induced by neighboring nuclei are operative and T2 becomes significantly shorter than T1.

In *solids* T2 is usually so short that the signal has died out within the first millisecond, whereas in fluids the magnetic resonance signal may last for several seconds. To a large extent, this is the cause of the low or absent signal from solid structures such as compact bone or tendons in medical magnetic resonance imaging.

With increasing field strength, T2 first increases as does T1. Then, while T1 still increases, T2 stays constant (on a plateau) but it might also appear to decrease.

This could be due to microscopic susceptibility differences which can induce a T2* effect.

So, if we represent T1 and T2 versus the microscopic mobility of the spin system, we will obtain for T1 a curve passing through a minimum, corresponding to the Larmor frequency, and a continuously decreasing curve for T2 (Figure 04-15).

At low and medium fields, the T2 value is approximately 3 seconds and the T1/T2 ratio is 1 for pure water. The T1 value of tissues is usually under 1 second. Here, the T1/T2 ratio increases rapidly with values of 5-10 covering most tissue types. It is about 5 for muscle tissue at 0.1 T.

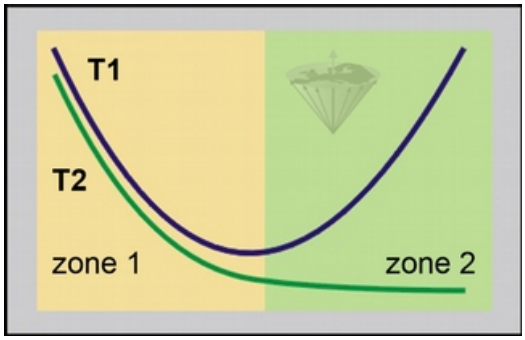

Figure 04-15:
Zone 1: high mobility with fast molecular motion; usually small molecules and 'free' water.
Zone 2: low mobility with slow molecular motion; usually large molecules and 'bound' water.

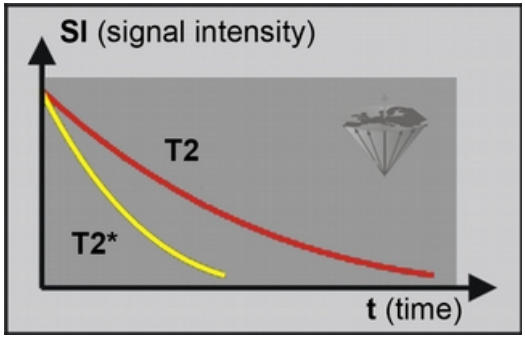

Figure 04-16:
T2 and T2*. The signal decay of T2* is faster than that of T2, because of field inhomogeneities and chemical shifts. However, the T2* can be made reappear by applying a second RF pulse.

In practice, it is observed that the same sample can show two different T2 relaxation times at the same field strength. This is because two phenomena contribute to the local inhomogeneity experienced by the nuclei:

- static and oscillating fields locally induced by neighboring magnetic moments (from other nuclei or unpaired electrons), and
- imperfections of the main static magnetic field B_0 (field inhomogeneities).

This leads to a decay of the observed signal which is faster than T2. It is called *T2* (T-two star)* (Figure 04-16). T2 has an irrecoverable decay whereas T2* has a recoverable decay and is always shorter than T2.

It is important to understand that T2* is not a constant or pure relaxation process. It should not be used for quantitative diagnostic purposes. It is a fluctuant time (or time range) for loss of phase coherence among spins oriented at an angle to the static magnetic field and depends on the location of the molecule in the magnet. These inhomogeneities can easily change, in MR imaging for instance if the patient moves or turns.

T2* is not a real relaxation parameter of the nucleus, it is a capricious global parameter – a comparison: each of one thousand tuning forks of the same type (frequency) vibrating while dephasing have their sound decaying slower than the global sound perceived. The main parameters contributing to T2* are spin-spin interactions, magnetic field inhomogeneities, magnetic susceptibility, and chemical shift effects.

For a given experiment (a single examination) T2* can be calculated in a similar way as T1 of complex systems (see the container example, Figure 04-06) by adding the R2 relaxation rates.

The observed decay rate R2* (R2* = 1/T2*) thus is related to the true spin-spin relaxation rate R2 (R2 = 1/T2) and to that induced by the field inhomogeneities $R2_{inh}$ or R2' ($R2_{inh} = 1/T2_{inh}$):

$$\mathbf{R2^* = R2 + R2_{inh}} \quad \text{or}$$
$$\mathbf{R2^* = R2 + R2'} \quad \text{or}$$
$$\mathbf{R2^* = R2 + \gamma \Delta B_0}$$

where γ is the gyromagnetic ratio (unit: MHz/T), ΔB_0 the difference in strength of the locally varying field (unit: T).

In case the signal is influenced by flow or perfusion, this has to be taken into account additionally, leading to an apparent T2 value: $T2_{app}$.

To remove the effect of field inhomogeneities, a spin echo (SE) can be used; its amplitude depends on the time, TE, which has elapsed since the initial excitation.

This is done in one of the formerly most common imaging sequences, the spin-echo pulse sequence, which was the standard pulse sequence in magnetic resonance imaging and the mainstay of clinical diagnosis. Even after the introduction of specialized pulse sequences for distinct diagnostic questions, SE remains the pulse sequence of preferred use if any doubt exists.

T2 on the Macroscopic Scale

To recapitulate: the T2 relaxation time is the the characteristic time constant for loss of phase coherence. The x-y magnetization will decay so that it loses 69% of its initial value in a time T2.

To measure this time, one specific radio frequency pulse sequence is preferred: the *spin-echo (SE) sequence*.

The Spin Echo Sequence

Let's look at this sequence first by comparing it with an example from everyday life – a race: After the spin system (e.g., the protons in a human body) has been excited by a 90° pulse, the spins dephase in the x'-y' plane. They separate from each other and fan out, some moving faster, others moving slower. If, after a time delay τ, the system is exposed to a 180° pulse, a refocusing is initialized. Now the faster spins lie behind the slower ones, but they catch up, which leads to an echo at time $TE = 2\tau$.

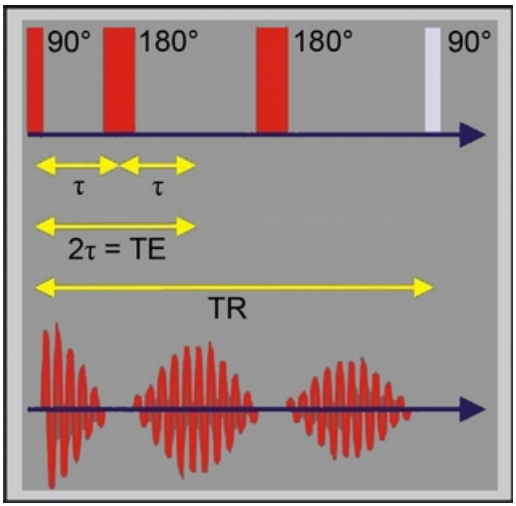

Figure 04-17:
Spin-echo pulse sequence. The spin system is excited by a 90° pulse. After a time delay (τ), one or several 180° pulses follow. This leads to the formation of an echo. The time between the 90° pulse and the peak of the echo is the echo time TE (= 2τ). TR is the repetition time between two complete pulse sequences.

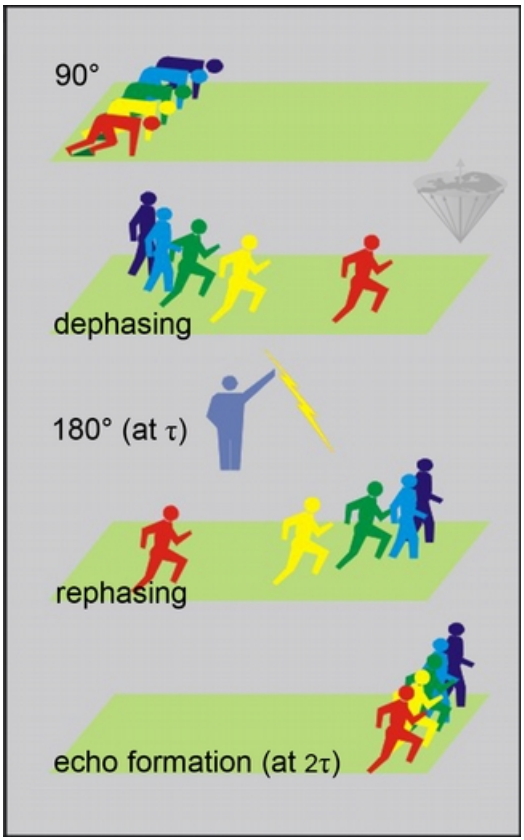

Figure 04-18 (right):
Spin-echo pulse sequence.: The race example.

The echo formation in a spin-echo pulse sequence can be compared with a race. At the time of the 90° pulse, all runners are lined up at the starting line. After the 90° pulse, the faster runners separate from the slower runners (dephasing).

At a certain time during the race, the runners are transposed (at the time τ when the 180° pulse is transmitted). Now the faster runners are behind the slower ones, but they catch up.

All reach the finishing line together (i.e., create an echo at the echo time 2τ = TE) (Figures 04-17 and 04-18).

The 180° pulse changes the phase of each spin by 180°; that is, it reverses its phase.

The position of the spins has not changed, so they will continue to rotate in the same direction.

However, the 180° pulse causes the spins to return towards their starting point (alignment), rather than rotating further away from it as shown in Figure 04-19.

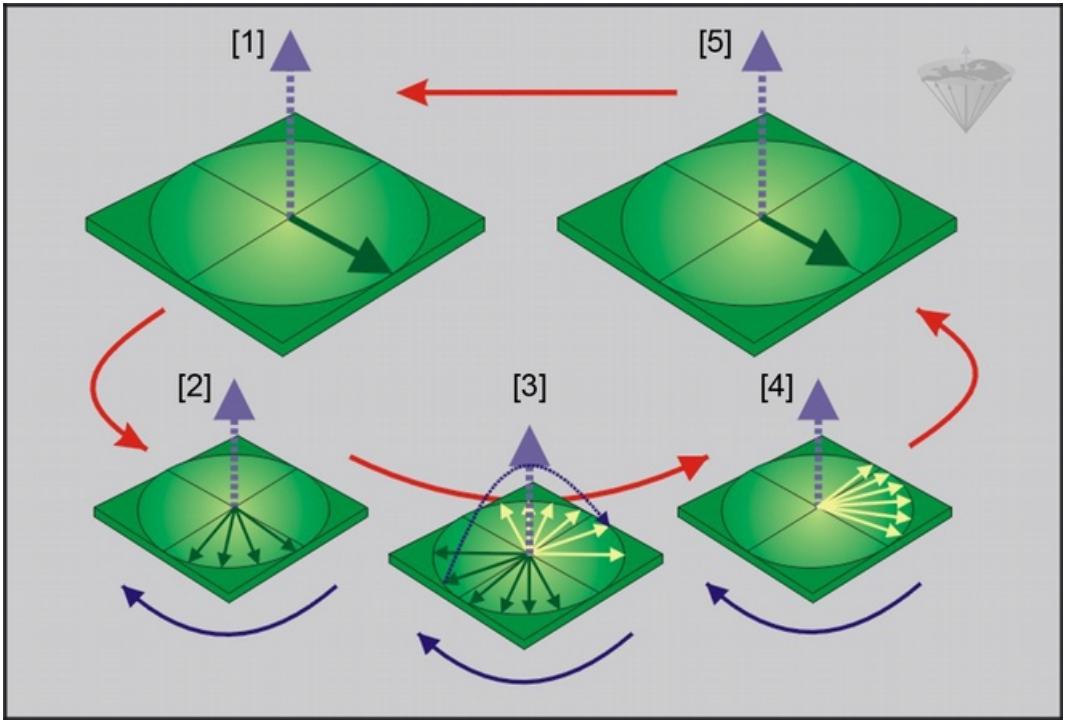

Figure 04-19:
After the system has been excited by a 90° pulse **[1],** the spins dephase **[2];** the system is exposed to a 180° pulse, the spins are refocused **[3]**. Now the faster spins are behind the slower ones **[4],** but they catch up with them, and create an echo at TE **[5].** Because there is a certain loss, the echo is smaller than the original signal.

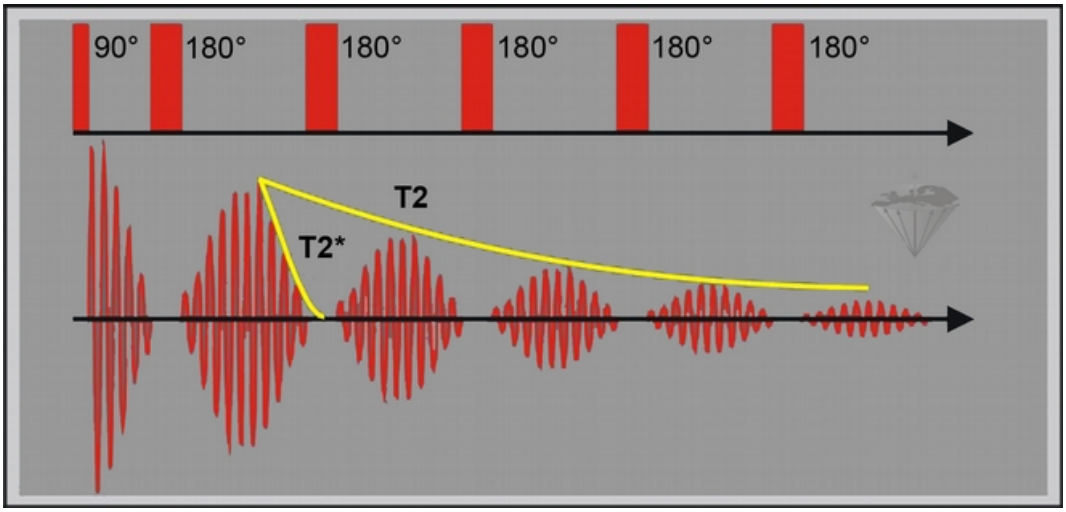

Figure 04-20:
The value of T2* can be obtained from the FID of single echoes while T2 is calculated from the peaks of the echo amplitudes. Several 180° pulses create echoes of decreasing amplitude (multiecho sequence). The envelope curve drawn through their peaks is the T2 decay curve.

If several 180° pulses are transmitted, echoes of decreasing amplitude are created. This is described as a multiple spin-echo or multi-echo sequence (Figure 04-20), commonly dubbed after its inventors the Carr-Purcell spin echo sequence[28], later modified as the Carr-Purcell-Meiboom-Gill (CPMG) sequence[29].

T2 is reflected by the envelope of the peaks of the echoes. At the center of the echo, the effects of inhomogeneities are cancelled out. Since the maximum amplitude of the echoes is not dependent on inhomogeneities and static gradients, echo amplitudes truly mirror the spin-spin relaxation of the sample. Flow or diffusion irreversibly bring the spins from one location to another, and so lead to an attenuation of the echo.

The decay after the 90° pulse and on either side of the center of the spin echo is governed by T2* rather than T2. Therefore, the signal decays rapidly away from the echo center.

At ultrahigh fields (3 Tesla and higher), one observes a substantial field-dependent reduction in apparent T2 values caused by dynamic dephasing effects.

28 Carr HY, Purcell EM. Effects of diffusion on free precession in nuclear magnetic resonance experiments. Phys Rev 1954; 94: 630-638.

29 Meiboom S, Gill L. Proton relaxation in water. Rev Sci Instrum 1958; 29: 688.

Practical Measurements of T1 and T2

Relaxation times can be measured in different ways with various degrees of accuracy.

I*n vitro* Determination

High-resolution magnetic resonance spectroscopists have measured T1 values since the middle of the last century. *In vitro* measurements are done on a small samples, approximately 0.1-1.0 ml or slightly larger in volume, in an extremely homogeneous magnetic field.

A variety of methods has been developed to obtain maximal precision with minimal time consumption. Typically, 15 to 30 magnetization measurements are performed on the sample for different time delays, TI in inversion-recovery experiments or TR in partial saturation experiments. Based on these results, an observed T1 value is calculated, and the error limits are usually better than 5%.

T2 can be calculated with a single multi-echo sequence. The more echoes one uses, the more accurate the measurement will be.

Calculations based on fast pulse sequences (so called '*black box'* sequences other than IR or SE) lead to rough estimates of T1, T2, T2* (and proton density) values.

They might be 'reproducible' when repeated, but the use of relaxation time values acquired with such pulse sequences is not advisable for scientific or clinical comparisons.

In vivo Determination

Magnet systems with larger bores allowed the examination of whole organisms, animals, and people, and a more physiological determination of relaxation time values than those of excised organs or tissues.

Relaxation time measurements were considered very important during the first years of commercial MR imaging. All machines were programmed to create true T1 and T2 images (i.e., T1- and T2 mapping), based on SE and IR sequences.

Very early, test objects and the protocols for their use to allow the measurement of T1 and T2 precision and accuracy were introduced in the framework of an extensive European project. The findings were sobering, but scientifically predictable. [30]

In particular, the accuracy and precision with which the relaxation times T1 and T2 could be measured from the images were found to be rather disappointing. Smaller comparison studies followed. It became clear that relaxation time values were not the claimed invaluable addition to diagnostics, and this "standard" application was skipped. [31]

A similar multi-center trial was repeated more than 30 years later. Phantom studies – newly introduced in the United States –

30 Anonymous. Protocols and test objects for the assessment of MRI equipment. EEC Concerted Research Project. Magn Reson Imaging. 1988; 6(2): 195-199.

31 Lerski RA, McRobbie DW, Straughan K, Walker PM, de Certaines JD, Bernard AM. Multi-center trial with protocols and prototype test objects for the assessment of MRI equipment. EEC Concerted Research Project Magn Reson Imaging. 1988; 6(2): 201-214.

described the same imprecision and irreproducibility of T1 measurements acquired on different MRI machines, most pronounced when rapid techniques for the estimation of relaxation constants were used (cf. page 89). [32]

Localization

One of the major problems of *in vivo* relaxation time measurements is the localization of the volume to be observed.

Actual accuracy of *in vivo* measurements depends on the number of points acquired and the quality of localization.

Localization is relatively uncomplicated in little or non-moving organs such as the brain, but demanding and partly impossible (in particular at high/ultrahigh fields) in organs with complex movement patterns such as the heart.

Details of localization techniques are given in Chapter 6.

Relaxation Time Values and Proton Density Calculation

The current most dependable method used to obtain a T1 image (T1 map), i.e., an image whose picture elements represent pure T1 values, relies on a mathematical manipulation of separately obtained images with different T1 influence. Measurements are easier and more accurate at low and medium fields, because T1 values are shorter, ECG triggering is less complicated, and artifacts less pronounced at these fields.

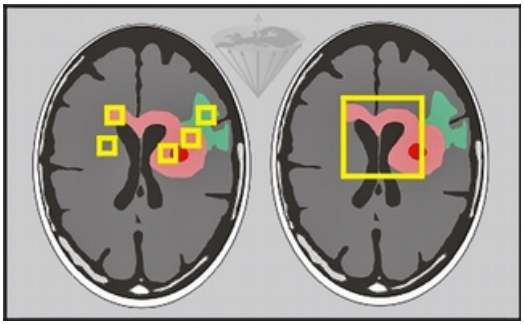

Figure 04-21:
Relaxation time measurements *in vivo* can be performed pixel by pixel and by regions of interest of different size. **Left:** Small regions of interest covering edema (green), tumor (pink), necrosis (red), etc. **Right:** Large region covering the entire tumor.

Typically, two to four images are used and the signals mathematically processed to calculate pure T1 values. Bearing in mind that *in vivo* relaxation can be multiexponential, it is somewhat inadequate to perform the analysis by such a limited fit to an exponential curve.

T2 images are calculated from the images of a multi-echo series, e.g. CPMG. In clinical settings, usually four or eight echoes are applied.

Diffusion, flow, and multiexponential decays are hardly ever taken into account in the fits and noise as well as motion artifacts add to inaccuracies.

Matrix size and slice thickness as well as partial volume effects are limiting factors in relaxation-time measurements *in vivo*. Partial volume effects and other factors influence the measurements. Variations within the same lesion related to vascularity, necrosis, and cell behavior (macroscopic compartmentalization) contribute to the overlapping of relaxation times values.

32 Keenan KE, Gimbutas Z, Dienstfrey A, et al. Multi-site, multi-platform comparison of MRI T1 measurement using the system phantom. PloS ONE. 2021; 16(6): e0252966. https://doi.org/10.1371/ journal.pone.0252966

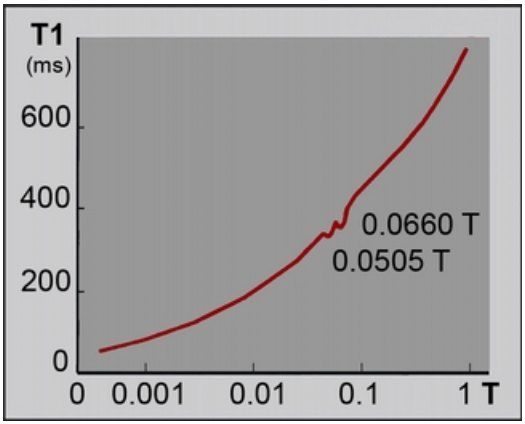

Figure 04-22:
The dispersion of T1 in tissues (ms) versus field strength (log Tesla) is not as monotonic and smooth as shown e.g. in Figure 04-04 and Figure 10-16.
This high resolution nuclear magnetic relaxation dispersion (NMRD) curve of a multiple sclerosis tissue sample reveals two dips (quadrupolar dips) at 0.0505 and 0.0660 T (2.1 and 2.8 MHz) where the otherwise steady increase of T1 is interrupted.

All methods relying on slices through the examined object will have as additional error source partial volume effects from the edges of the slices; the only method which avoids this slice problem is the true 3D volume imaging method.

Standard deviation in fitting, artifacts, and variations in the selection of volume elements by the operators are all possible sources of error (Figure 04-21).

Furthermore, similar lesions may have a more than single exponential relaxation rate, e.g., brain tumors and multiple sclerosis plaques. This is not unexpected, considering the heterogeneous nature of tumors – and tissues in general.

Reproducibility of such measurements is also limited.

The multilayered complexity of factors and features influencing and creating relaxation time and proton distribution changes is not completely understood yet.[33]

A simplified view offered by Koenig suggests that water molecules can wander rather extensively by thermally-induced diffusion throughout the intra- and extracullular regions of tissue, and that the exploration is rather thorough in a time of the order of T1 (or even T2).

Another concept is the highly structured water, restrained for a significant time in a geometry defined by various ionic and molecular constituents of the cytoplasm.[34]

However, some features of the T1-dispersion do not fit easily into these concepts, for instance cross relaxation phenomena that lead to quadrupolar dips in the T1-dispersion plot. They are dependent on field strength and temperature (Figure 04-22).[35]

More about the dependence of relaxation times on static field strength and its influence upon contrast can be found in Chapter 10.

33 Springer Jr. CS, Li X, Tudorica LA, Oh KY, Roy N, Chui SYC, Naik AM, Holtorf ML, Afzal A, Rooney WD, Huang W. Intratumor mapping of intracellular water lifetime: metabolic images of breast cancer? NMR Biomed 2014; 27: 760–773.

34 Koenig SH Brown III RD. The importance of the motion of water in biomedical NMR. in: Rinck PA, Muller RN, Petersen SB. An introduction to biomedical nuclar magnetic resonance. Stuttgart, New York: Thieme Publishers. 1985; 50-58.

– Koenig SH. Theory of relaxation of mobile water protons induce by protein NH moieties, with application to rat heart muscle and calf lens homogenenates. Biophys J. 1988; 53(1): 91-96.

35 Rinck PA, Fischer HW, Vander Elst L, Van Haverbeke Y, Muller RN. Field-cycling relaxometry: medical applications. Radiology 1988; 168: 843-849.

Figure 04-23 (top):
Top row: Images of a patient with a polyp in the left paranasal sinus. **Bottom row:** images of a cervical spine. **(a)** Calculated (pure) T1, and **(b)** calculated (pure) T2 image. Figures **(c)** and **(d)** show T1- and T2-weighted images. Pure T1 and T2 images are of very limited diagnostic value. Multiparameter weighted images are far more valuable for clinical diagnosis and commonly used in patient studies.
Simulation software: MR Image Expert®

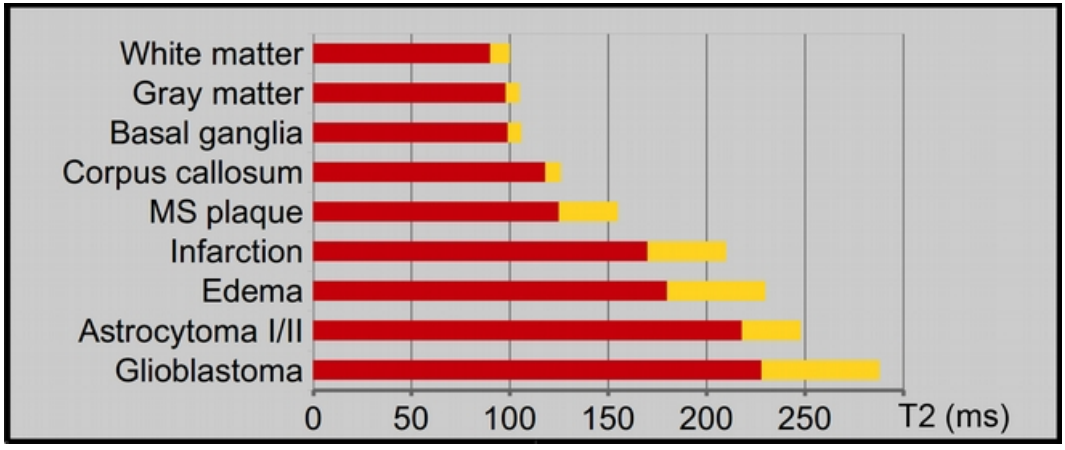

Pure T1/T2 Images versus T1- / T2-Weighted Images

Relaxation time and proton density values can be used to create synthetic or simulated images for training and teaching purposes.

In clinical routine, people often talk about T1, T2 or proton-density images. The correct terms are T1-weighted, T2-weighted, and proton density (ρ)-weighted (or better, intermediately weighted) images, because these images have only a certain T1, T2, or proton-density dependence.

However, they are not calculated pure relaxation time or proton density images. Chapter 10 will explain this in detail.

Figures 04-23c and d are T1-weighted and T2-weighted images, to be compared with the pure T1 and T2 images of Figure 04-23a and 04-23b.

Figure 04-24 (left):
T2 values of normal and pathological human brain tissues measured at 0.15 Tesla, based upon 24 echoes. The standard deviation (SD) is given in yellow. The SD of normal tissues can reach 20%, that of pathological tissues 30%.

Relaxation Times Blues

If the scientific details of this chapter were too boring, get the Blues – an excursion into the background and history of T1 and T2:
To be read on page 97.

Measurements in Medical Diagnostics

Fifteen years after the first description of different relaxation behavior in tissues by Erik Odeblad,[36] other researchers started postulating that relaxation times differentiate tumors from normal tissue since most T1 (and in a similar way T2) values of pathologic tissue can differ markedly from the T1 of the similar normal tissue[37] (cf. Chapter 20: History of MRI).

However, the ability to discriminate, type, or even grade tumors using relaxation time values has remained a dream, despite the sophisticated multi-point fits introduced over the years. Figure 04-24 shows that there are differences between, in this case, T2 of normal and diseased tissues.[38] Although values of T2 are more accurate than those of T1 because more points are used for their calculation, these differences are not significant between T2 values of, for instance, tumors and edema or infarction.

Every year, the literature announces new attempts to exploit relaxation-time measurements *in vivo*. There are some positive reports about its successful use. Most concern follow-up of therapy, with patients being their own reference.

36 Odeblad E, Lindström G. Some preliminary observations on the proton magnetic resonance in biological samples. Acta Radiol 1955; 43: 469-476.

37 Damadian R. Tumor detection by nuclear magnetic resonance. Science 1971; 171: 1151-1153.

38 Rinck PA, Meindl S, Higer HP, Bieler EU, Pfannenstiel P. Brain tumors: detection and typing by use of CPMG sequences and in vivo T2 measurements. Radiology 1985; 157: 103-106.

Publications include, for instance, the report that relaxation times from leukemic bone marrow can be used for the differential diagnosis of this disease (Figure 04-25).[39] Similar results in high-grade gliomas have been published by another research group.[40]

Yet, the follow-up of treatment based upon relaxation-time values is difficult and in most instances dubious (Figure 04-26). A rise and subsequent decline of relaxation time values after a local intervention might rather indicate edema and inflammation than successful treatment.[41]

Several other studies dealt with pixel-by-pixel mapping of relaxation times of normal appearing white brain matter in multiple sclerosis (MS) patients. The results suggested minute invisible changes in the white matter which might explain brain function deficits that cannot be explained by the size and location of visible MS plaques.[42, 43, 44] However, also these measurements are not clinically applicable.

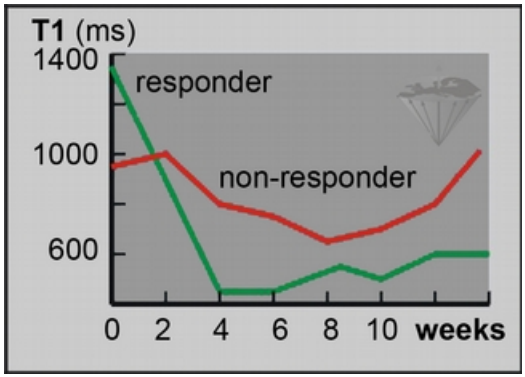

Figure 04-25:
T1 measurements. Follow-up of treatment of acute myeloblastic leukemia. Responder: green; non-responder: red.

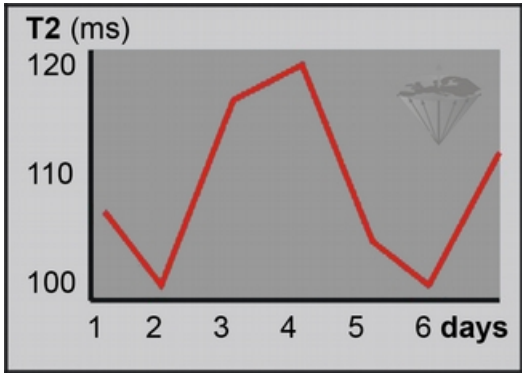

Figure 04-26:
Relaxation-time measurements of identical samples under identical measurement conditions can reveal great standard deviations, as shown in this example. Relying on *in vivo* measurements to evaluate the outcome of treatment is dubious. Only in some instances do massive changes allow a positive assessment.

39 Jensen KE, Sorensen PG, Thomsen C, Christoffersen P, Henriksen O, Karle H. Prolonged T1 relaxation of the hemopoietic bone marrow in patients with chronic leukemia. Acta Radiol 1990; 31: 445-448.

40 Boesiger P, Greiner R, Schoepflin RE, Kann R, Kuenzi U. Tissue characterization of brain tumors during and after pion radiation therapy. Magn Reson Imaging 1990; 8: 491-497.

41 Zhang X, Zhang F, Lu L, Li H, Wen X, ShenJ. MR imaging and T2 measurements in peripheral nerve repair with activation of Toll-like receptor 4 of neurotmesis. Eur Radiol 2014; 24: 1145–1152.

42 Barbosa S, Blumhardt LD, Roberts N, Lock T, Edwards RH. Magnetic resonance relaxation time mapping in multiple sclerosis: normal appearing white matter and the 'invisible' lesion load. Magn Reson Imaging 1994; 12: 33-42.

43 Lacomis D, Osbakken M, Gross G. Spin-lattice relaxation (T1) times of cerebral white matter in multiple sclerosis. Magn Reson Med 1986; 3: 194-202.

44 Rinck PA, Appel B, Moens E. Relaxationszeitmessung der weissen und grauen Substanz bei Patienten mit multipler Sklerose. RöFo - Fortschr Röntgenstr 1987; 147: 661-663.

Availability of databases of *in vivo* relaxation-time measurements is very limited. A large collection of data was published by Bottomley et al.[45]

A comparison between *in vivo* and *in vitro* relaxation measurements is quite difficult because many T1 relaxation time values change rapidly after excision. Only brain tissues reveal a relatively stable relaxation behavior after they have been removed from the body.[46]

After absolute T1 and T2 values had been used unsuccessfully by researchers, combinations of T1 and T2, histogram techniques, and sophisticated three dimensional display techniques of factor representations were used ('fingerprinting', biomarkers; cf. Critical Remarks at the end of this chapter).[47]

45 Bottomley PA, Foster TH, Argersinger RE, Pfeifer LM. A review of normal tissue hydrogen NMR relaxation times and relaxation mechanisms from 1-100 MHz: dependence on tissue type, NMR frequency, temperature, species, excision, and age. Med Phys 1984; 11: 425-448.

– Bottomley PA, Hardy CJ, Argersinger RE, Allen-Moore G. A review of 1H nuclear magnetic resonance relaxation in pathology: are T1 and T2 diagnostic? Med Phys 1987; 14: 1-37.

46 Fischer HW, Van Haverbeke Y, Rinck PA, Schmitz-Feuerhake I, Muller RN. The effect of aging and storage conditions on excised tissues as monitored by longitudinal relaxation dispersion profiles. Magn Reson Med 1989; 9: 315-324.

– Fischer HW, Rinck PA, van Haverbeke Y, and Muller RN. Nuclear relaxation of human brain gray and white matter: analysis of field dependence and implications for MRI. Magn Res Med 1990; 16: 317-334.

47 Skalej M, Higer HP, Meves M, Brückner A, Bielke G, Meindl S, Rinck P, Pfannenstiel P. T2-Analyse normaler und pathologischer Strukturen des Kopfes. Digit Bilddiagn 1985; 5: 112-119.

Rapid Relaxation Constant Estimation Techniques

Precise measurements require long acquisition times; the repetition time, TR, should be equal to or greater than 5×T1. At 0.15 T, the T1 of myocardium is around 380 ms, at 1.5 T it has climbed to around 1000 ms. Measurements at low fields take approximately 5 minutes, at high or ultrahigh field more than 10, perhaps 15 minutes. Thus, makeshift faster acquisition methods were sought and developed.

Fast acquisition of quantitative T1 maps can, e.g., be based on a series of snapshot fast low-angle shot (FLASH) images after inversion of the magnetization.[48] Such techniques were for instance used for estimating the concentration of paramagnetic contrast agents in an organ.

Since the acquisition of quantitative tissue data from a beating heart has to be very fast, lately much research is focused on modifications of a pulsed NMR sequence proposed by David C. Look and Donald R. Locker in 1969.

MRI did not exist at that time, and Look and Locker used their time-saving one-shot method for NMR spectroscopy instead of the conventional methods to measure the T1 relaxation time. The spectroscopic "LL" method was within 10% of the conventionally precise-calculated value.[49]

48 Deichmann R, Hahn D, Haase A. Fast T1 mapping on a whole-body scanner. Magn Reson Med 1999; 42: 206-209.

49 Look DC, Locker DR. Pulsed NMR by toneburst generation. J Chem Phys 1969; 50: 2269-2270.

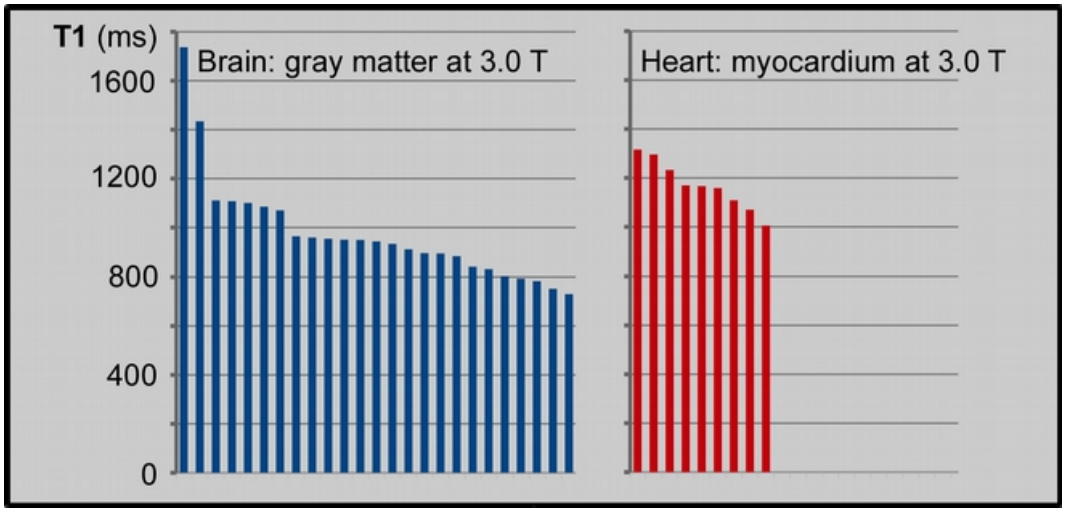

Figure 04-27:
T1 values at 3 Tesla of human gray brain matter (25 different collectives) and myocardium (9 different collectives) measured *in vivo* on different MR machines with accelerated data acquisition algorithms (compiled from different sources). The estimated values are imprecise and spread across several hundred milliseconds.

In the 1980s, the method was further developed for MRI by Graumann and his colleagues.[50] Others followed and precision was waived for speed. Among the modified sequences for cardiac and, e.g., brain MRI experimentally (and sometimes clinically) used today, one finds PURR,[51] MOLLI,[52] and ShMOLLI.[53] They all suffer to varying extent from errors, resulting in an underestimation of the true T1. 'Apparent' T1 values of MOLLI and ShMOLLI measurements of, e.g., normal myocardium have an error range of 30% or higher and always are shorter than true T1 values.

A number of different pulse sequences, e.g., SASHA, SAPPHIRE, DESPOT and many others were also introduced and tested. Unfortunately, none of these values are reliable or reproducible (Figure 04-27).[54]

50 Graumann R, Barfuss H, Fischer H, Hentschel D, Oppelt A. TOMROP: a sequence for determining the longitudinal relaxation time T1 in magnetic resonance tomography. Electromedica 1987; 55: 67-72.

51 Lee JH. PURR-TURBO: a novel pulse sequence for longitudinal relaxographic imaging. Magn Reson Med. 2000; 43:773-777.

52 Messroghli DR, Radjenovic A, Kozerke S, Higgins DM, Sivananthan MU, Ridgway JP. Modified Look-Locker inversion recovery (MOLLI) for high-resolution T1 mapping of the heart. Magn Reson Med 2004; 52: 141–146.

53 Piechnik SK, Ferreira VM, Dall'Armellina E, Cochlin LE, Greiser A, Neubauer S, Robson MD. Shortened modified Look-Locker inversion recovery (ShMOLLI) for clinical myocardial T1-mapping at 1.5 and 3 T within a 9 heartbeat breathhold. J Cardiovasc Magn Reson. 2010; 12: 69. 1-11.

54 Bojorquez JZ, Bricq S, Acquitter C, Brunotte F, Walker PM, Lalande A. What are normal relaxation times of tissues at 3 T? Magn Reson Imaging. 2017; 35: 69-80.

From a scientific point of view, these measurements are unsound because the margin of error is huge (cf. page 83).

The sharp fall of T2* values at high and ultrahigh fields is related to the drastic rise of magnetic susceptibility effects which grow linearly with magnetic field strength; pure T2 is not affected in the same way.

Imperfect spoiling of transverse magnetization at higher flip angles in gradient echo sequences has a negative effect on a precise estimation of signal intensity and other parameters, such as relaxation times.[55]

Critical Remarks

Yet, in the end, it is not even the most elaborate data acquisition that makes typing of normal and pathological tissues ('fingerprinting') or grading of diseases impossible but rather the complexity of tissue composition and the overlapping of relaxation time values of heterogeneous volume elements examined and processed into a single number or number range.

It is helpful to once look into a microscope and to see how complex and complicate tissue structures are, both in normal and in pathological tissues – and in not-normal, but not (yet) pathological tissues.

Even following a trend of changing T1 and T2 acquired with the same equipment and the same imaging parameters to calculate the relaxation constant values during and after the treatment of a patient can be like "fishing in troubled waters."

From a scientific point of view, MR imaging is a crude and not very exact technology. However, to be imprecise in medicine does not preclude specific use.

One example is the measurement of cardiac iron overload, which according to a number of cardiological publications is, so far, one of the most useful diagnostic approaches in patients with thalassemia major; however, many papers about the topic are dubious and the methods used lack scientific background. Myocardial damage in thalassemia is induced by iron deposition: free unbound iron catalyzes the formation of cell-toxic hydroxyl radicals. Thus, monitoring of myocardial iron content would be useful and could be done by estimating T2 or T2*.

To be able to discriminate 'normal' myocardium and pathological tissue alteration the approach requires massive tissue changes, and it cannot distinguish between fibrosis, inflammation, and infiltrative cardiomyopathies, myocardial edema and possible other tissue changes. However, the pathological T2* values seem to be highly reproducible on different MR equipment.[56]

Another area of application of relaxation times measurements might be the follow-up of massive T1 changes after the injection of a targeted contrast agent, such as Mn-DPDP and the comparison of plain and contrast-enhanced tissue, e.g., in heart diseases (cf. page 250 and Figure 13-17a).

Here, too, imprecise measurements might be of diagnostic value.

55 Zur Y, Wood ML, Neuringer LJ. Spoiling of transverse magnetization in steady-state sequences. Magn Reson Med. 1991; 21: 251–263.

56 Auger D, Pennell DJ. Cardiac complications in thalassemia major. Ann N Y Acad Sci 2016; 1368: 56-64 [review].

Biomarkers. To add confusion to complicated science, changes of terms and terminology are common in contemporary bioscience.

Thirty years after the description of relaxation times and relaxation rates as possible or, rather, questionable biological indicators they were re-ranked among *biological markers* or *biomarkers*.

In general, biomarkers are biological indicators of any kind; there are thousands of them. They are not specific for MR imaging or MR spectroscopy. Typical biomarkers are measurements or scores such as blood pressure, body temperature, the body mass index, or clinical signs such as external manifestations of disease. Many of them are helpful, others of limited and questionable value – still widely used.

In MR imaging, biomarkers break down into numerous subgroups where they can be applied standing alone or several combined, relaxation times being only one of them. Aside of T1 and T2, there are other possible indicators for the detection, diagnosis, and monitoring of treatment, i.e., of particular physiological or disease states.

Quantification of MR parameters is also discussed in Chapter 15. Biomarkers extracted through image segmentation and multispectral analysis are also described in Chapter 15, those acquired with the help of contrast agents in Chapter 13, and by dynamic imaging in Chapter 16.

Terminology and Understanding the Fundamentals. Some physicians and researchers are using 'apparent' T1 for *cardiac mapping* and mix T2* (in reality $T2_{app}$), R2* and r2* randomly.

In some publications, additional terms are also used wrongly or confusingly, for instance T1* (a term which is not appropriate because T1 is not affected by susceptibility effects) for an apparent T1 ($T1_{app}$ or $T1_{influx}$).

Details on the correct use of terms can be found on page 79.

The Author

Peter A. Rinck is a University Professor of Radiology and Magnetic Resonance (*emeritus*) and has a Doctorate in History of Medicine.

After a classical school education he attended medical school in Berlin (Free University of Berlin) and served his internship and residency in radiology, nuclear medicine and radiation therapy at Charlottenburg University Hospital in Berlin.

Afterwards, until 1983, he was involved in the very early development of magnetic resonance imaging as Senior Research Associate at the State University of New York at Stony Brook where he worked in Paul C. Lauterbur's research group (Nobel Prize in Medicine 2003). The first version of this textbook was written at this time.

Subsequently Rinck worked as physician-in-charge of one of the first two German government sponsored MR machines in Wiesbaden, Germany.

Between 1987 and 1994 he was head of Europe's biggest clinical and research MR facility – at that time – at the University of Trondheim, Norway. Between 1986 and 2012 he was also Adjunct Professor at the School of Medicine and Pharmacy of the University of Mons-Hainaut in Belgium.

Since 1982 Rinck is Chairman of the European Magnetic Resonance Forum, EMRF, and since 2008 President of the Council of The Round Table Foundation, TRTF.

He is also Chairman of the Selection Committees of the the Pro Academia Prize and of the European Magnetic Resonance Award.

Visiting Professorships: The Neurological Institute of Colombia. Bogotá, Colombia (1986); Charité University Hospital, Medical Faculty of Humboldt University, Berlin, Germany (1991-1992); et al.

President of the European Society for Magnetic Resonance in Medicine and Biology, 1985-1987; president of the annual meetings 1989, 2002. Scientific consultant and expert adviser to international organizations and foundations (among them WHO, European Commission, UNIDO, the Nobel Committee). Honorary, founding, or ordinary member of numerous professional and learned societies.

Among others, awards and prizes from the Alexander von Humboldt Foundation, Max Kade Foundation, NATO, European Commission, Fonds National de la Recherche Scientifique de Belgique, the Research Council of Norway, and German Research Society (DFG).

Author and/or editor of several books – not only scientific or medical – an e-learning website, numerous papers in refereed journals and communications to international scientific meetings; and since 1990 *Rinckside* (learned columns).

Acknowledgements

There has been a long list of contributors to this and earlier versions, among them Atle Bjørnerud, Patricia de Francisco, Jürgen Hennig, Richard A. Jones, Jørn Kværness, Willy Eidsaunet, Robert N. Muller, Gunvor Robertsen, Timothy E. Southon, and Geir Torheim.

Their support, ideas, dedication, and feedback have added much to the quality of this work.

We are also indebted to our friends who took care of some of the translations of the printed version – among them Andrea Giovagnoni for the Italian edition, Valentin Sinitsyn for the latest Russian edition, Luis Martí-Bonmatí and Ángel Alberich-Bayarri for a Spanish e-learning version; and Song Yingru for an earlier Chinese edition. The Editor-in-Charge of the current Chinese e-Learning and book editions is Qiuju Zhou.